



HAL
open science

Acoustic monitoring of timber structures: Influence of wood species under bending loading

Marianne Perrin, Imen Yahyaoui, Xiaojing Gong

► To cite this version:

Marianne Perrin, Imen Yahyaoui, Xiaojing Gong. Acoustic monitoring of timber structures: Influence of wood species under bending loading. *Construction and Building Materials*, 2019, 208, pp.125-134. 10.1016/j.conbuildmat.2019.02.175 . hal-02123152

HAL Id: hal-02123152

<https://hal.science/hal-02123152v1>

Submitted on 22 Oct 2021

HAL is a multi-disciplinary open access archive for the deposit and dissemination of scientific research documents, whether they are published or not. The documents may come from teaching and research institutions in France or abroad, or from public or private research centers.

L'archive ouverte pluridisciplinaire **HAL**, est destinée au dépôt et à la diffusion de documents scientifiques de niveau recherche, publiés ou non, émanant des établissements d'enseignement et de recherche français ou étrangers, des laboratoires publics ou privés.



Distributed under a Creative Commons Attribution - NonCommercial 4.0 International License

1 **Acoustic monitoring of timber structures: influence of wood** 2 **species under bending loading**

3 Marianne Perrin^{1*}, Imen Yahyaoui¹, Xiaojing Gong¹

4 ¹Institut Clément Ader (ICA), Université de Toulouse, CNRS UMR 5312, 1 rue Lautréamont, 65000
5 Tarbes, France

6 *e-mail: marianne.perrin@iut-tarbes.fr (corresponding author)

7 Declarations of interest: none

8 **Abstract**

9 The use of wood in civil engineering structures, such as timber bridges, has been increasing in recent
10 years. Unfortunately, our knowledge of their behaviour towards sustainability problems is far from
11 complete and it is necessary to develop monitoring techniques like acoustic Emission (AE) that allow
12 early identification of pathologies. This study focuses on the analysis of the influence of wood species
13 on the acoustic response under bending loading. *The results of this experimental study show a*
14 *correlation between AE signal features and certain failure mechanisms but also that these acoustic*
15 *signatures are different for each timber species.*

16 **Keywords:** Timber structures, Acoustic Emission monitoring, Damage acoustic signature, Structural
17 Health Assessment

18 **1. Introduction**

19 Today, the use of wood is becoming more and more widespread in the field of construction [1]. Wood
20 is a renewable resource with low energy consumption that traps CO₂ during the life of the structure.
21 Although the use of wood is an ecological solution, the integration of this material into structures
22 remains limited because of its complex behaviour (strong anisotropy, heterogeneity, sensitivity to
23 variations of humidity and temperature, limited mechanical properties, etc.). In order to overcome
24 these limitations, hybrid structures have been developed in recent decades. In this context, timber-
25 concrete bridges have been built in France. Examples include the Vallon bridge at Riou de Lantosque,
26 the bridge of Cognin, and the bridge at Lure [1]. In addition, the European project NR2C (New Road
27 Construction Concept), devoted to the bridges of the future, has demonstrated the mechanical interest

28 of new wood / concrete / composite decks [2]. These multi-material wood-based structures are both
29 original and mechanically promising but the fact that this type of construction is still recent can result
30 in some misunderstanding of their mechanical behaviour [3].

31 As a safety measure and to be able to anticipate and optimize the maintenance operations of these
32 structures, it is interesting to detect and identify the severity of damage from its initiation. In this
33 context, it is necessary to use a non-destructive test method to evaluate and assess the health of a
34 structure and to predict the evolution of the damage. Acoustic emission (AE) seems an interesting
35 technique for this purpose since it allows the response of the structure to mechanical or environmental
36 constraints to be followed continuously. In addition, AE also enables early detection of evolving
37 defects and the localization of acoustic sources as well as the characterization and identification of
38 various mechanisms of damage [4]. Although the characterization of the damage mechanisms of
39 composite materials or cementitious materials by AE is now widely reported [5], [6], [7], [8], few
40 studies have concerned wood material. Most of the work identified in the literature shows that the
41 anatomical structure of wood has a significant influence on its acoustic response under mechanical
42 loadings [9], [10], [11], and Chen [12] also observed that the acoustic activity rate was proportional to
43 the damage rate of wood. More recent work has partially correlated acoustic signatures to a particular
44 kind of damage [13], [14], [15]. These works are generally limited to a specific wood species
45 subjected to a particular type of stress and the assignment of acoustic signatures is often based on
46 hypotheses.

47 The research work we present here focuses on the influence of the wood species on the acoustic
48 response of wood material. In order to work on one of the most frequent stresses identified on timber
49 structures [16], only the bending stress is considered. First, we will focus on the evolution of damage
50 at different stages of loading through a conventional analysis of acoustic activity. Then we will
51 identify the acoustic signature of the different damage mechanisms for the three species through a
52 multi-variable analysis coupled with video tracking. The evolution of diagnostic methods and signal
53 processing algorithms, coupled with the cross-use of several control techniques, makes it possible to
54 increase the robustness and richness of the acoustic data. In addition to an easier correlation between
55 the mechanisms of damage and the acoustic signatures, these developments give a better

56 understanding of the damage scenarios and the parameters influencing them, which will allow us to
57 establish a comparison of the acoustic responses among individual species.

58

59 **2. Materials and testing methods**

60 2.1. Wood species

61 Four-point bending tests were carried out on 3 different species: two softwoods, Douglas fir
62 (*Pseudotsuga Menziesii*) and Silver fir (*Abies Pectinata*), and a hardwood species, Poplar (*Populus*
63 *Negra*). For the three species, the tests were performed on samples cut from the same board to limit the
64 impact of inter-species heterogeneity and 5 samples were tested for each species. All species of wood
65 are characterized by a heterogeneous structure and different properties in the longitudinal (L), radial
66 (R) and tangential (T) directions [17]. Douglas fir was chosen because it is currently the species most
67 commonly used in construction thanks to its remarkable mechanical characteristics and its natural
68 durability properties. One of the peculiarities of Douglas fir is that its growth rings are very apparent,
69 as the Late Wood (LW) is much denser and more colourful than the Early Wood (EW) [16] (Table 1).
70 The second species selected was Silver fir, another resinous species, which has the particularity of
71 being a very abundant local species in the south-west of France and which is not sufficiently
72 developed today from a commercial point of view. Its structure and heterogeneity are different from
73 those of Douglas fir. For example, the Silver fir has much less marked annual rings. This results in
74 properties between the EW and the LW closer than for the Douglas fir (Table 1). The third species was
75 Poplar, a hardwood species. Its structure is much more homogeneous for a density relatively close to
76 that of the other two (Table 1). Thus, we can compare the behaviour of a homogeneous hardwood
77 species with the behaviour of two heterogeneous softwood species, these three species having
78 comparable density.

79 Table 1. Raw density of the species tested in this study (average of 5 samples), characteristics of LW
80 et EW [18] of the species.

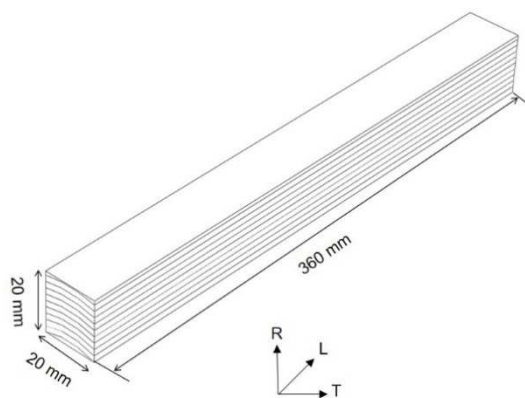
| Species | Raw density in kg/m ³ (variability) | Density | | Young Modulus (GPa) | |
|-------------|---|---------|------|---------------------|-------|
| | | EW | LW | EW | LW |
| Douglas fir | 498.6 (±6.3%) | 0.29 | 0.82 | 18.24 | 45.51 |
| Silver fir | 424.3 (±8.2%) | 0.27 | 0.62 | 20.50 | 28.25 |
| Poplar | 408.1 (±2.7%) | 0.4 | 0.48 | - | - |

81

82
83
84

2.2. Mechanical four-point bending test

85 The tests conducted and monitored by AE were based on standardized tests (NF B- 51-008 [19]). All
86 of them were performed on an MTS 20/M electromechanical testing machine with a maximum
87 capacity of 100 kN. Before each test, the specimens used were conditioned in a climatic chamber at 20
88 °C and 65% relative humidity (NF B51-002 [20]) until mass stabilization. The dimensions of the
89 specimens were 360 mm (L) x 20 mm (R) x 20 mm (T) (Figure 1).

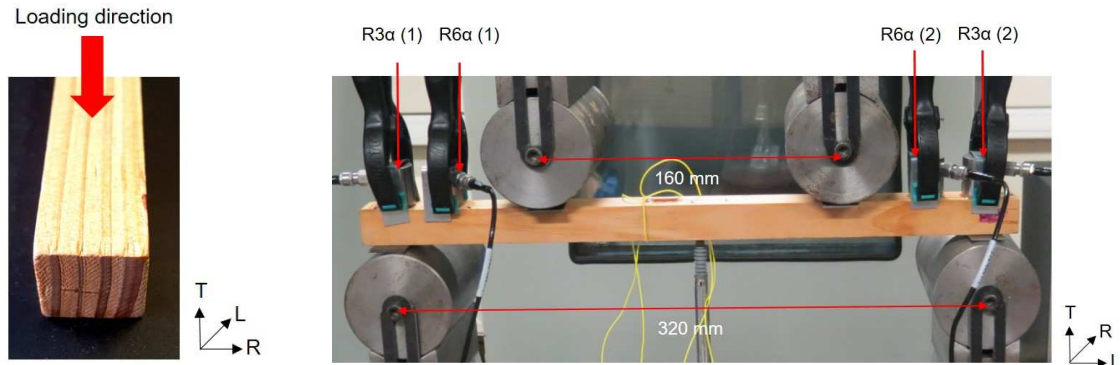


90
91
92
93

Figure 1: Bending test specimen dimensions according standard NF B 51-008[19]

94 In order to ensure that the Early Wood and the Late Wood are loaded in the same way, the standard
95 NF B 51-008 [19] requires a load to be applied parallel to the annual rings (Figure 2a). The bending
96 tests were also carried out in imposed displacement mode, using a speed of 4 mm / min in accordance
97 with NF B 51-008 [19]. It should be noted that a steel wedge was positioned between the supports and
98 the sample in order to limit local indentation (Figure 2b).

99 Each test was tracked by AE and video tracking using a Canon PowerShot SX40 HS camera, with a
100 sampling rate of 24 frames per second and a resolution of 1920*1080 pixels.



(a)

(b)

Figure 2: Four-point bending test procedure (a) Loading direction (b) Sensor positions.

101
102
103
104
105
106
107

2.3. AE instrumentation

108 The choice of instrumentation is essential in AE. Most studies use sensor ranges having resonant
 109 frequencies that are typically between 150 kHz and 450 kHz [9], [10], [14], [15], [21], [22], [23].
 110 However, wood is a very dispersive material, particularly because of its heterogeneity. The
 111 propagation of acoustic waves within the wood material is accompanied by large attenuation, which
 112 can reach 1 dB / cm [23], [24], [25]. It is thus necessary to select a sensor that collects the maximum
 113 of signals during the damaging of the wood material. Several authors have shown that the signals
 114 emitted in the wood are of rather low frequency [21]. A previous study, published in TAMAP [26],
 115 shows that the frequencies emitted during mechanical tests are lower than 100 kHz. In order to cover
 116 the entire frequency range identified, the different tests were instrumented via two types of sensors:
 117 R6 α and R3 α (MISTRAS Group), which have resonance frequencies of 60 kHz and 30 kHz,
 118 respectively. The coupling of the sensors on the specimen is performed via a silicone grease and their
 119 fixation is guaranteed by the use of metal brackets and clamps (Figure 2b). The coupling is then
 120 checked by Hsu-Nielsen tests [27]. Each sensor was connected to a 40 dB pre-amplifier and then
 121 connected to the acquisition system (PCI8 board from MISTRAS Group). Concerning the positioning
 122 of the sensors, following a series of preliminary tests and in order to continue to determine the location
 123 of the acoustic events for as long as possible during the tests, the R6 α and R3 α sensors were placed on
 124 the top of the test piece (Figure 2b). The fact that the main damage occurs on the side under tensile

125 load of the specimen would have implied a very rapid loss of location if the sensors had been placed
126 below the test piece. The precise position of the sensors is shown in Figure 2b.

127 2.4. Tuning the acquisition parameters

128 The acquisition threshold of the system was chosen according to the signal-to-noise ratio. It was set at
129 35 dB for all tests. Analogue filters were used to eliminate unwanted mechanical noise: high pass
130 filter: 20 kHz, low pass filter: 400 kHz. In addition, following the preliminary tests, the values chosen
131 for the time windows in order to identify the individual acoustic hits correctly were: **Peak Definition**
132 **Time: 40 μ s, Hit Definition Time: 200 μ s, Hit Lockout Time: 300 μ s.**

133 2.5. Statistical treatment of data

134 The AE signals were then analysed using an Unsupervised Pattern Recognition (UPR) technique with
135 the NOESIS software (Enviroacoustics SA) to group signals with a similar acoustic signature. This
136 type of statistical analysis is widely described in the literature [28], [29]. In this study we kept the
137 maximum of AE features in order to obtain the most robust signal classification possible. These
138 parameters were: rise time, counts, counts to peak, absolute energy, duration, amplitude, average
139 frequency, frequency centroid, initiation frequency, reverberation frequency, and peak frequency.
140 Naturally, in order to limit the weight of certain parameters in the analysis, a normalization of the data
141 between 0 and 1 was carried out. After a comparative study of the various classification algorithms at
142 our disposal, the k-means algorithm was used to classify the signals into different groups. The number
143 of groups was validated through 2 statistical criteria: the Davies & Bouldin (D&B) coefficient [28]
144 and the Tou coefficient [30].

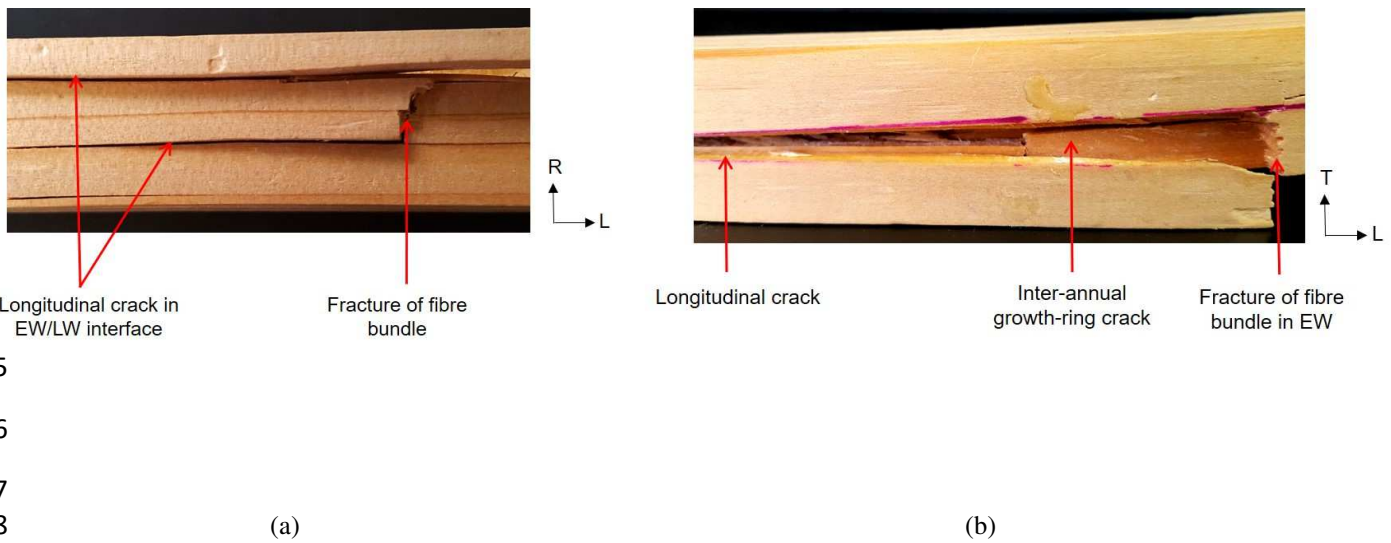
145

146 **3. Results and discussion**

147 3.1. Bending tests on Douglas fir

148 The five specimens of Douglas fir responded similarly to the bending tests. Failure surfaces showed a
 149 simple tensile fracture mode [31], [32]. The results presented here are those of a specimen
 150 representative of the general behaviour observed on the batch of specimens (Figure 3). The fracture
 151 surfaces showed numerous cracks at the EW/LW interfaces (Figure 3a) as well as large areas of
 152 longitudinal cracks (Figure 3b). The detachment of one or more initial wood bundles was also widely
 153 observed (Figure 3b) (one bundle corresponds to all the fibres of one or more growth rings).

154



160 Figure 3: Observations of the Douglas fir specimen (a) tension face (LR view)
 161 (b) Side view (TL view)

162
 163

164 Images from the video permitted visual and audio analysis of the damage during the bending test.
 165 Many audible noises (unaccompanied by visible damage) could be identified at specific times during
 166 the test, as well as some macroscopic damage. Table 2 presents the significant moments.

167

168 Table 2: Record of feature points on video recording.

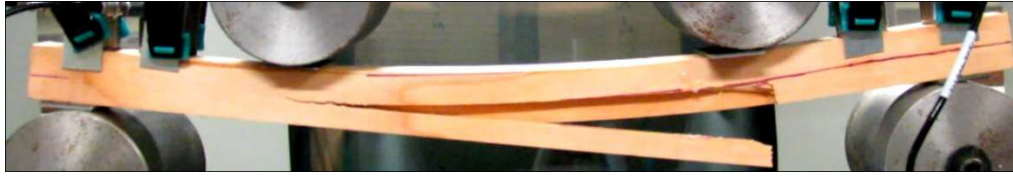
169

| Hit number (Figure 5) | Time (s) | Observation/listening |
|-----------------------|----------|---|
| 1 | 131.5 | Audible noise (no visible damage) |
| 2 | 147.8 | Audible noise (no visible damage) |
| 3 | 152.6 | Audible noise with macroscopic rupture (Figure 4 a) |
| 4 | 154 | Audible noise with macroscopic rupture (Figure 4b) |
| 5 | 159.2 | Audible noise (no visible damage) |

170

171 Figure 4 shows the two instances of macroscopic damage observed during the test.

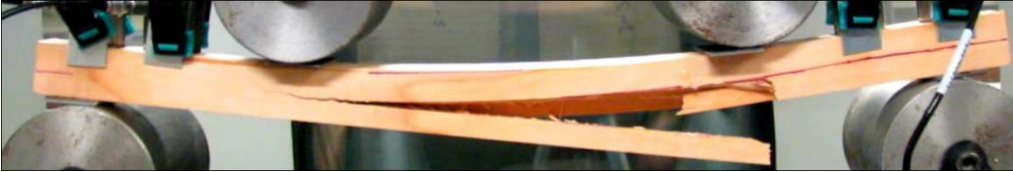
172



(a)

173

174



(b)

175

176

177

178

Figure 4: (a) First macroscopic fracture (b) second macroscopic fracture

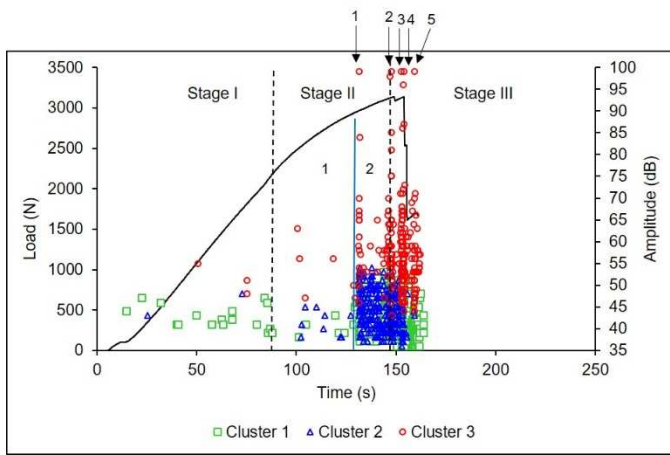
179 These two occurrences of macroscopic damage were generated by the zones of cracking between the
180 different rings, and also by the breaking of bundles of fibres and the propagation of cracks in the
181 longitudinal direction. The pull-out of a bundle of fibres, as during damage occurrences 3 and 4, was a
182 brutal mechanism (fibre breakage then crack propagation).

183 These characteristic moments were also identified on the recording of the associated acoustic activity.
184 Figure 5a shows this activity collected on the sensor that recorded the most hits. Three distinct stages
185 can be observed. The first stage corresponds to the linear part of the Load-time curve. It is
186 characterized by the detection of acoustic signals of amplitude not exceeding 55 dB. The second stage
187 begins when the Load-time curve begins to become non-linear and ends at the point where the load is
188 highest. In terms of acoustic response, this stage can be divided into two parts. During Part 1, the
189 acoustic activity undergoes a small increase and the amplitude does not exceed 65 dB. Part 2 starts at t
190 $= 131.5$ s with an audible noise. It is characterized by an increase in the number of hits together with
191 the recording of high amplitude signals (99 dB). The third stage corresponds to the rupture stage. In
192 terms of acoustic response, the number of hits continues to increase very significantly. The
193 multiplicity of sources of acoustic emission appears clearly in Figure 5a, where a very broad spectrum
194 of amplitudes, ranging from 35 dB to 99 dB, is observed.

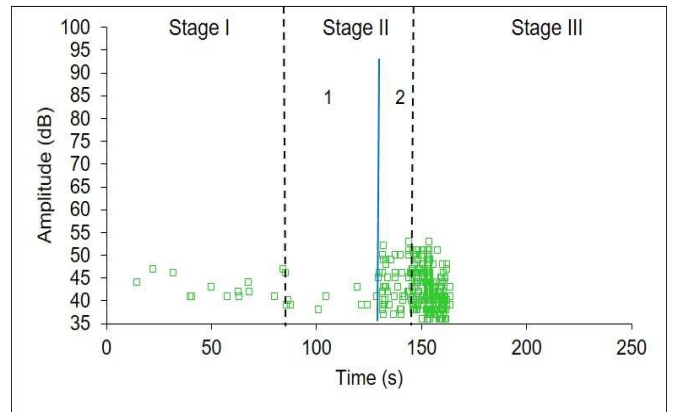
195 The statistical classification of the signals, based on the k-means algorithm and validated by the
196 coefficients of Davies & Bouldin and Tou, presented 3 clusters of significantly different signals. The
197 first cluster (Figure 5b) contained 44% of the signals. This cluster appeared early during the test then

198 intensified from 148.7 s, when a peak load was recorded. In addition, cluster 1 was clearly visible at
 199 the time of the two macroscopic breaks. The second cluster (Figure 5c) contained 35% of the signals.
 200 Few signals appeared before 131.5 s. Then the appearance of this cluster of signals intensified. It
 201 should be noted that the increase in the activity density of the second cluster was consecutive to the
 202 first audible signal at 99 dB. This cluster of signals also ended early compared with the other two
 203 clusters. The third cluster (Figure 5d) included 21% of the signals and started to appear significantly as
 204 audible noises began to be emitted (131.5s).

205



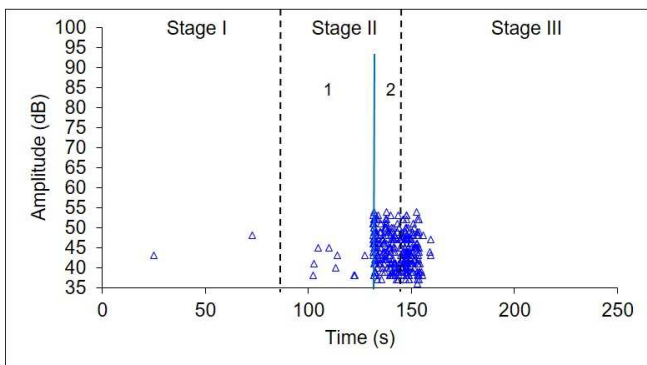
206



207

(a)

(b)



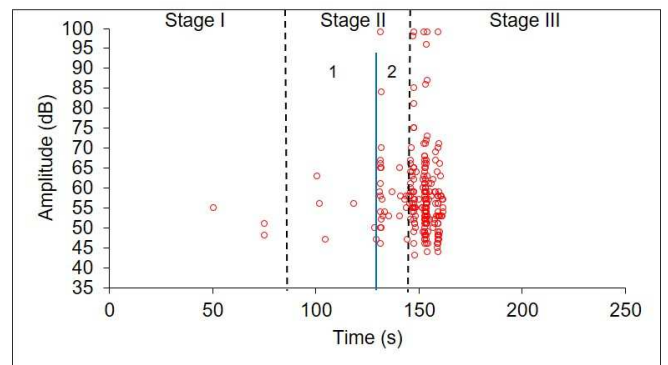
208

209

210

(c)

(d)



211 *Figure 5: AE activity for the Douglas fir specimen during the 4 point bending test, (a) evolution of signal*
 212 *amplitude and load (b) cluster 1, (c) cluster 2 (d) cluster 3*

213

214

215 Following the analysis of the video data and the associated acoustic activity, a damage scenario was
216 developed, allowing each signal cluster to be associated with a specific damage mechanism. From the
217 beginning of the first audible noises at $t = 131.5$ s, the acoustic activity increased, in particular in the
218 second cluster of signals. High amplitude (99 dB) signals were synchronized with audible breakage
219 sounds. This means that, from $t = 131.5$ s, wood fibres started to break. Following these first breaks,
220 mobility mechanisms were set up in the shear planes, leading to cracks between the EW/LW rings.
221 Thus, from 131.5 s, a significant amplification of the second cluster of signals was observed. The
222 evolution of the damage resulted in breakage of wood bundles for $t = 152.6$ s and $t = 154$ s,
223 accompanied by a significant increase in the first and third clusters of signals. This macroscopic
224 damage was the consequence of fibre breaks in the tensile zone being transformed into longitudinal
225 propagation when a singularity was encountered in the specimen. This damage scenario based on
226 visual observations correlated with the acoustic activity made it possible to label the three clusters of
227 signals. The first cluster was associated with the macroscopic failure mechanisms observed at 152.6 s
228 and 154 s. These signals were related to the coalescence and propagation of longitudinal microcracks
229 at the beginning of the test and then to the longitudinal propagation of macroscopic cracks in stage III.
230 The second cluster of signals corresponded to the inter-laminar shear mechanisms at the EW / LW
231 interfaces. These mechanisms created signals of low amplitude and low energy. The most energetic
232 signals (cluster 3) were synchronized with the audible sounds of fibre breaks and thus ultimately
233 associated with breaks in fibre bundles.

234

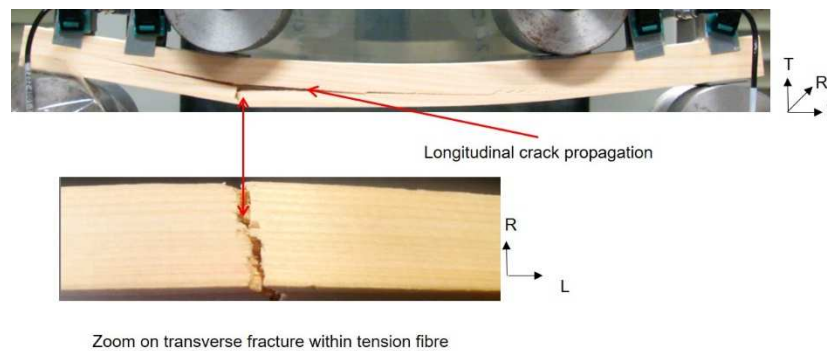
235 3.2. Bending tests on Silver fir

236 The mechanical response of the five test pieces of Silver fir to the bending stresses was similar to
237 that of the Douglas fir but the ruptures observed on the specimens of Silver fir were sudden with little
238 prior warning. The final rupture of the specimen began in the tension region by the propagation of a
239 transverse crack in mode I (opening crack), followed by a longitudinal propagation in modes I + II
240 (opening and shearing crack) until the final failure (Figure 6).

241

242

243



244

Figure 6: Fracture surfaces observed on Silver fir specimen.

245

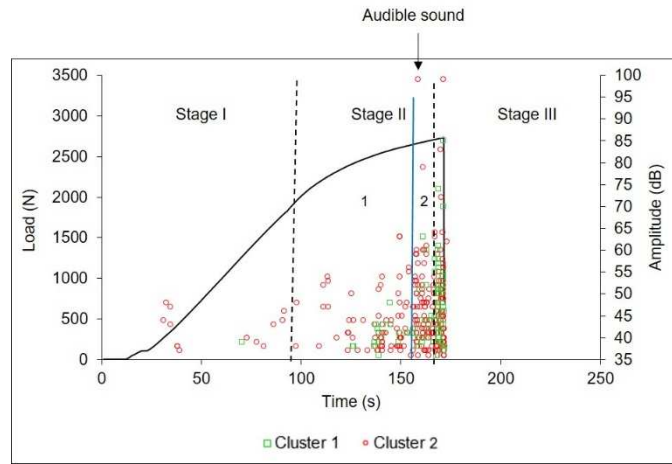
246

247 The video follow-up showed no precursors to the failure of the specimen, except a fibre rupture noise
248 at $t = 158.6s$. As in the Douglas fir bending tests, the acoustic activity collected on the Silver fir
249 presented three different stages. The number of hits cumulated in the first stage evolved in a regular
250 manner (Figure 7a). The amplitude of recorded signals did not exceed 50 dB. In terms of acoustic
251 response, the second stage could be divided into two parts according to the acoustic activity rate
252 recorded. Amplitudes in stage II-1 did not exceed 65 dB (Figure 7a). Stage II-2 began with the
253 recording of a high amplitude signal (99 dB) at $t = 158.6s$. The last stage was almost instantaneous. At
254 the acoustic response level at this time, the hit amplitude (Figure 7a) covered the entire range from the
255 lowest to the highest amplitude (from 35 dB to 99 dB). There was also a huge increase in the number
256 of hits.

257 The ranking obtained by the k-means algorithm is presented in Figure 7. The number of signal clusters
258 validated by the statistical criteria of Davies & Bouldin and Tou was two.

259 The first cluster (Figure 7b) contained 24% of the signals. It started relatively late in the test. There
260 was an increase in activity at the time of the final rupture. The second cluster (Figure 7c) contained
261 76% of the signals. The average amplitude of the signals of the second cluster was small. It was also
262 noted that the amplitudes increased as the rupture phase approached.

263



264

265

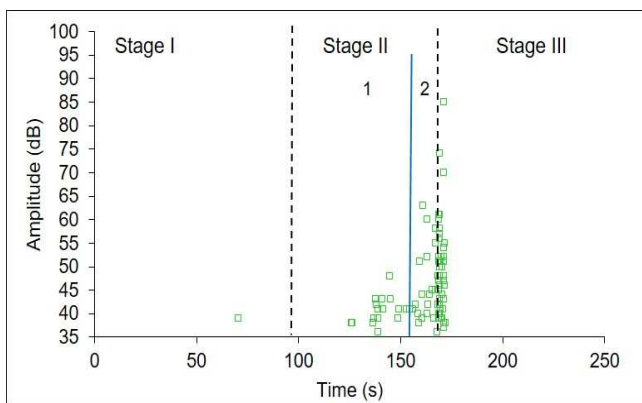
266

267

268

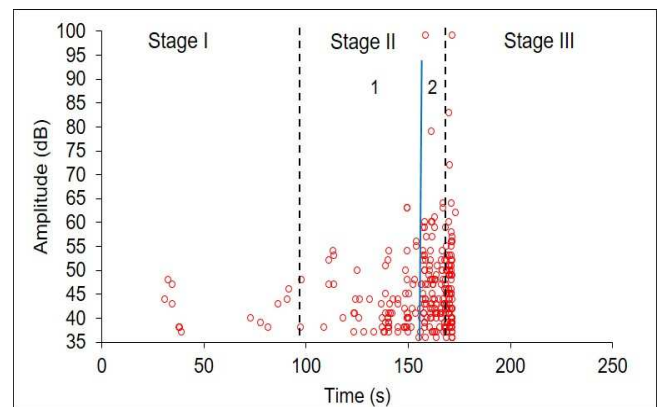
269

(a)



270

(b)



(c)

272 *Figure 7: AE activity for the Silver fir specimen during the 4 point bending test, (a) evolution of signal amplitude*
 273 *and load (b) cluster 1, (c) cluster 2.*

274

275 To label the two clusters of signals dissociated by multi-variable statistical analysis, we mainly relied

276 on the correlation between the acoustic emission and the film record. The first cluster began in stage II

277 with coalescence and propagation of longitudinal microcracks. Then, in the rupture stage (stage III),

278 the signals of the first cluster corresponded to the propagation of the longitudinal crack in mode I + II

279 (opening and shearing crack) identifiable on the lateral face of the specimen (Figure 6). The second

280 class of signals represented a progressive phenomenon that started very early in the test. The

281 mechanism of damage present at that time was the transverse microcracking that started during stage I.
282 The propagation and the coalescence of these transverse microcracks led to the mode I breakdown of
283 fibres over the full width of the tensile part of the specimen. The audible noise specific to fibre breaks
284 identified at the beginning of stage II-2 corresponded to the high amplitude signals of the second class.
285

286 3.3. Bending tests on Poplar

287 Poplar specimens showed a combined failure mode (simple traction and bevel propagation) that
288 started in the tensile zone of the specimen. The fracture surfaces presented in Figure 8 is representative
289 of the behaviour of Poplar under bending stress. Crack initiations were located in the area of minimum
290 stiffness lying under the top loading supports, where a zone of matting that weakened the material was
291 observable (Figure 9). Under the effect of the bending stress, the two cracks propagated in mixed
292 mode I + II (opening and shearing crack) crosswise towards the centre of the specimen. The fracture
293 surfaces on the broken specimens formed a cross at (X). A major mechanism was observed on the
294 fracture surfaces of the specimen: an inclined cracking mechanism (mix of microcracks in several
295 planes of the sample).

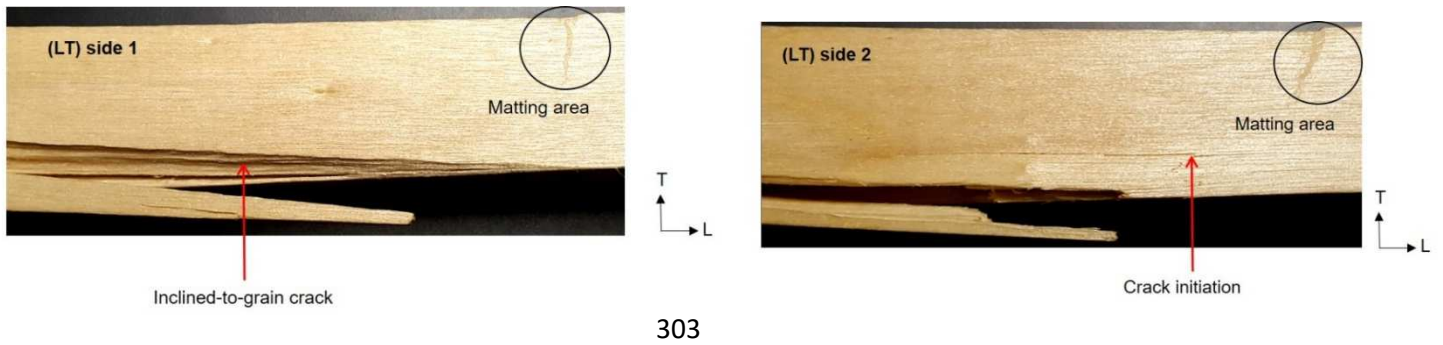


296
297 (a)



298
299 (b)

300
301
302 *Figure 8: Fracture surfaces observed on Poplar specimen (a) side view (LT view) (b) tension face (LR view).*



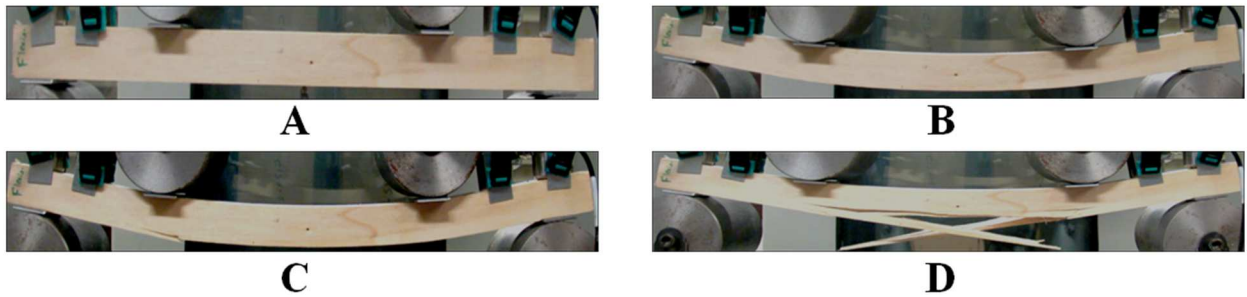
304

305 (a)

(b)

306 *Figure 9: (a) Front of the specimen (b) Rear face of the specimen.*

307 Four images corresponding to characteristic moments of the damage were extracted from the film
 308 (Figure 10). Images A and B, identified at different times during the test, showed no visible damage. It
 309 should be noted that image B corresponded to the moment of the first audible noise identified during
 310 the test. Image C showed the presence of macroscopic damage. This was a detachment of fibres,
 311 observed in the tension part of the specimen under the upper left loading support, followed by a crack
 312 propagation over a short distance. This first failure was followed by two other very rapid breaks that
 313 started simultaneously on the two opposite sides of the specimen (Figure 10 - image D).
 314

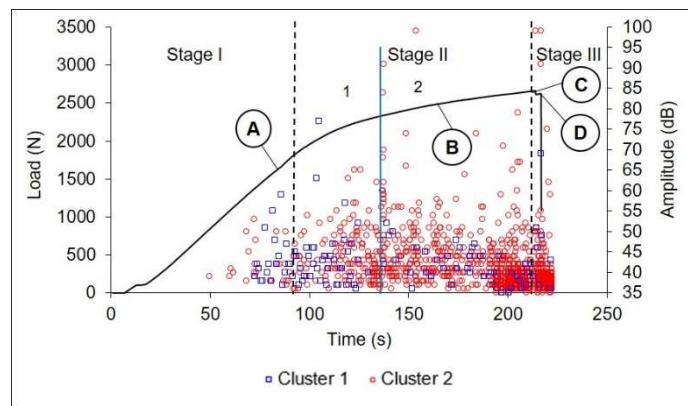


315 *Figure 10: Characteristic images of the poplar sample damage extracted from the film.*

316

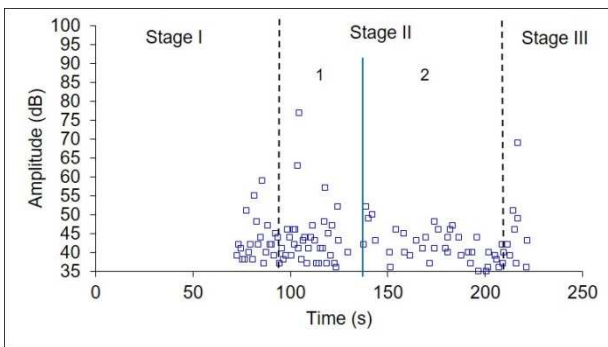
317 As for the two preceding species, three specific stages could be identified on the Load-time curve.
 318 Recording of acoustic hits started from $t = 50$ s. The number of cumulated hits (Figure 11a) was
 319 relatively small in this stage. The amplitude of the recorded signals varied between 35 dB and 55 dB
 320 (Figure 11). In terms of acoustic response, the second stage showed that the number of hits intensified
 as the test progressed. Figure 11 reveals two distinct parts in this second stage. In stage II-1, the

321 amplitudes remained modest (<60 dB) whereas, in stage II-2, a significant increase in amplitudes
 322 could be observed with signals exceeding 90 dB. We also noted a very significant increase in the
 323 number of hits around 200 s. The last stage was almost instantaneous. The amplitude of the recorded
 324 signals varied between 35 dB and 99 dB, and the number of high amplitude signals was relatively
 325 small.
 326 The results of the classification of acoustic signals by the k-means method are presented in Figure 11.
 327 Two different signal clusters were identified by the **Davies&Bouldin** and Tou criteria.

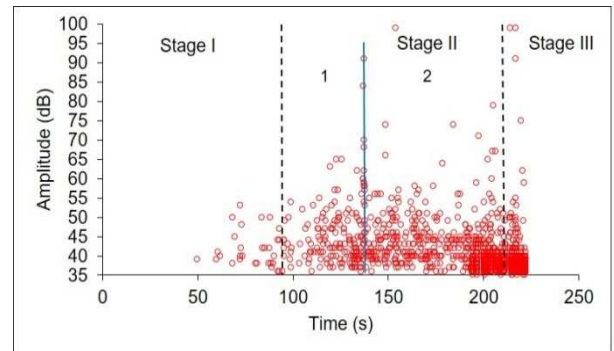


(a)

328
 329
 330
 331



(b)



(c)

332
 333
 334
 335
 336
 337
 338

Figure 11: AE activity for the Poplar specimen during the 4-point bending test, (a) evolution of signal amplitude and load (information A, B, C and D refer to Figure 10) (b) cluster 1, (c) cluster 2.

339 Figures 11b and 11c show that the two clusters of signals evolved in particular ways. The first cluster
 340 (Figure 11b) contained only 5% of the signals. It appeared around 70 s and showed a homogeneous
 341 distribution of the signals throughout the test. The evolution of the second cluster of signals (Figure
 342 11c) was much more significant. The cluster contained 95% of the signals and started at 50s. It

343 showed weak activity in stage I, a progressive intensification in stage II and very intense activity at the
344 end of the test. It should be noted that the second cluster of signals included all the signals having high
345 amplitudes.

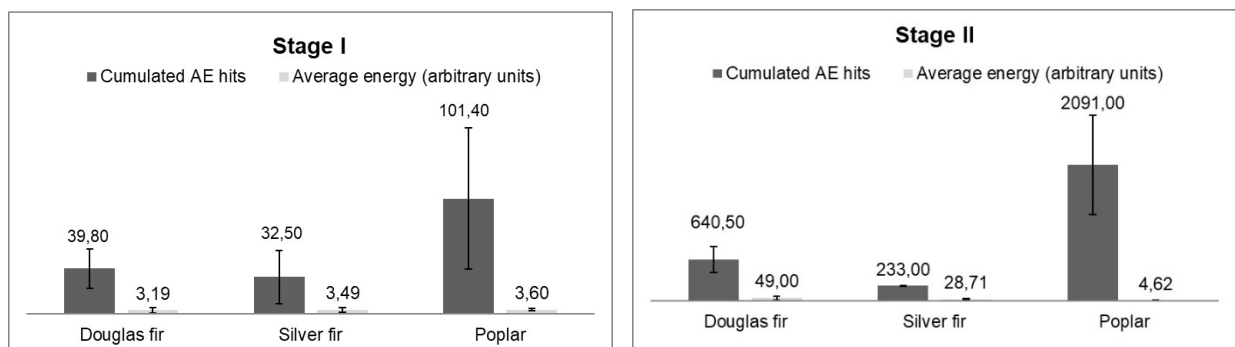
346 If we compare the observations made on the specimen and the evolution of the two clusters of signals,
347 it would seem that the first cluster of signals can be attributed to the permanent deformation in
348 compression obtained by the matting effect, *although we have no direct evidence* (Figure 9). This is a
349 local shear deformation of the fibres observed on all specimens of Poplar. This deformation does not
350 lead to any great damage, which explains why it generates only 5% of the signals. *The signals of the*
351 *second cluster correspond to* the different types of microfissuring (longitudinal and transversal) as well
352 as to the breaking of fibres, and this cluster includes almost all signals with disparate characteristics as
353 shown by the variety of amplitudes. The evolution of its activity during the *test is in line* with the
354 evolution of the damage. The signals detected during stage I *are generated* during the initiation of
355 microcracks, the coalescence and propagation of these microcracks occur in stage II and this activity
356 intensifies during stage II-2 as the propagation of microcracks begins to be accompanied by fibre
357 breaks. This is confirmed in stage III, with several high amplitude signals associated with a significant
358 acoustic activity between 35 and 50 dB. These signals come from macroscopic cracking and rupture of
359 the specimen.

360

361 3.4 Comparison of acoustic responses

362 The three species of wood studied in these works, stressed in bending, exhibit clearly
363 different behaviours with respect to their damage. One of the main reasons that can be
364 invoked concerns their anatomical structures. Several comparisons can be made, first of all by
365 comparing hardwood and softwood species. Several studies in the literature have shown that
366 softwood species are more emissive than hardwood species [10], [11], [21], [33]. We show
367 here that these results are to be taken with caution, as already found by Chen [12], since the
368 detection sensitivity of AE is largely dependent on the choice of instrumentation and
369 acquisition parameters. The analysis of our results indicates that the intensity of the acoustic

370 activity varies from one stage to another depending on the species. In stage I, we find that the
 371 two softwoods (Douglas fir and Silver fir) generate an equivalent number of signals (Figure
 372 12a). On the other hand, the Poplar generates at least three times more signals than the two
 373 softwoods (Figure 12a). Finally, if we compare the average energy of each hit, we can see that
 374 the AE of the Douglas fir, Poplar and Silver fir have comparable average energies. During
 375 stage II, the Poplar emits many more signals than the two other woods (Figure 12b). On the
 376 other hand, although the number of signals generated by the Poplar is more than three times
 377 that generated by the Douglas fir, the average energy released by the Poplar signals is ten
 378 times less than that generated by the Douglas fir. Regarding the Silver fir, the average energy
 379 released is approximately half that released by the Douglas fir. In stage III, the breaking stage,
 380 Poplar still generates lots of signals (Figure 12c). The small number of cumulated hits
 381 generated by the Silver fir during its damage reflects its instantaneous failure. Nevertheless,
 382 the average energy released is the largest of the three species. The average energy released by
 383 the second softwood species is slightly lower as that released by the Silver fir. In Poplar, the
 384 rupture stage is characterized by a large number of low energy signals.

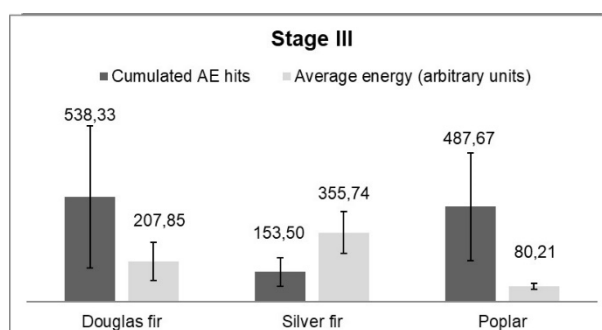


385

386

(a)

(b)



387

(c)

388

Figure 12: Comparison of the AE response of the three wood species during the three stages of loading

389

(a) stage I, (b) stage II (c) stage III (AE energy = $\int_T A. dt$).

390

391 The evolution of the number of hits and the energy released reflects the behaviour of the three

392 species when they are undergoing damage. Douglas fir shows a significant increase in energy

393 released in stage II. This is related to the specific mechanisms that are set up at the interfaces

394 between EW and LW. Douglas fir is one of the species where the heterogeneity between early

395 wood and late wood is strong [18]. For the Douglas fir, the density can differ by a factor of

396 three (0.82 for LW, 0.29 for EW) [18], which causes stress concentrations at the EW / LW

397 interfaces, thus establishing complex damage mechanisms. For the Silver fir, the density

398 differs only by a factor of 2.3 (0.62 for LW, 0.27 for EW) [18]. This may explain the

399 difference in behaviour under loading of the Silver fir, where there is almost no damage

400 between growth rings. The particularity of the Silver fir is the sudden release of energy at the

401 time of the breakage phase. Concerning Poplar, the differences between EW and LW are very

402 small, as shown by the density values: 0.48 for LW and 0.40 for EW [18]. Poplar is a diffuse

403 pore wood. EW and LW vessels have almost the same diameter and are evenly distributed

404 over spring wood and summer wood. Its relative homogeneity results in damage mechanisms

405 that are initiated quickly but evolve progressively until rupture, thus generating numerous but

406 not very energetic signals. One of the consequences of this is the difficulty of drawing up a

407 detailed classification of the different types of signals coming from Poplar.

408

409 **4. Conclusion**

410 The aim of this research work was to understand the differences in acoustic response

411 according to the wood species under bending stress.

412 Regarding the influence of wood species on the overall acoustic activity, we observed a
413 different behaviour that can be summarized as follows: overall, the hardwood species emitted
414 more signals than either of the softwood species, but the signals were of low energy. The
415 comparison between the two softwood species also showed different behaviours. The species
416 of Douglas fir was very emissive throughout the test while the Silver fir was characterized by
417 a very sudden break with very energetic signals at the end of the test. The statistical
418 classifications implemented during this study showed that three separate classes of signals
419 could be identified for Douglas fir (cracking at EW/LW interfaces, longitudinal cracking, and
420 fibre breakage). Only two mechanisms were observed and identified in the acoustic activity of
421 the Silver fir: longitudinal cracking and fibre breakage. For poplar, due to its relatively
422 homogeneous anatomical structure, the statistical processing of the data did not make it
423 possible to discriminate the signals coming from different damage mechanisms.

424 Our results show that a comparison of the acoustic behaviour of different wood species cannot
425 be limited to a simple analysis of the acoustic emissivity. The hardwood and softwood species
426 studied showed different behaviours not only in the number of hits emitted but also in the
427 energies released. On the other hand, the use of statistical processing of acoustic data coupled
428 with video tracking showed that certain specific mechanisms were responsible for the
429 differences in acoustic behaviour observed between species. This was the case, for example,
430 for cracking mechanisms at the EW / LW interfaces in the case of the Douglas fir, which
431 remains the species mainly used in the construction of wooden structures today. The
432 recognition of damage mechanisms through the recording of specific acoustic signals opens
433 up many interesting perspectives for the development of wood-based structures, in particular
434 with regard to the problems of maintenance of such structures. Before arriving at this stage, it
435 will nevertheless be necessary to be able in a short course to decorrelate the signals collected
436 from measurement biases (propagation, natural frequency of the sensor, etc.) that modify the

437 original acoustic source. This will make it possible to identify universal acoustic signatures
438 that are independent on the measurement systems and thus make the analysis of information
439 reliable. it will also have to be able to solve the problem of the transition from the laboratory
440 specimen to the actual structure. This involves solving the questions related to on-site
441 instrumentation but also the definition of relevant indicators to alert bridges managers. Not
442 only the experience gained on other types of structures [34], but also the improvement and the
443 miniaturization of the sensors and the electronics will certainly be necessary in order to
444 answer to these imperatives.

445 This research was funded by the French Ministry of Higher Education, Research and
446 Innovation.

447 **References**

- 448 [1] F. Renaudin, P. Jandin, Design of wood-concrete composite beams under deck bridge-
449 Theoretical developments and constructions examples, 3rd International conference on Timber
450 Bridges, Skelleftea, Sweden, 2017
- 451 [2] O. Ben Mekki, F. Toutlemonde, Experimental Validation of a 10-m-Span Composite
452 UHPFRC–Carbon Fibers–Timber Bridge Concept, *J. Bridge Eng.*, 16(1) (2011) 148-157.
453 [https://doi.org/10.1061/\(ASCE\)BE.1943-5592.0000114](https://doi.org/10.1061/(ASCE)BE.1943-5592.0000114).
- 454 [3] V.A. Trung Nguyen, Multi-renforcement du bois lamellé-collé – Etude théorique et
455 expérimentale, Doctoral Dissertation, Ecole Nationale des Ponts et Chaussées, Paris, France,
456 2010
- 457 [4] N. Godin, P. Reynaud, G. Fantozzi, Emission acoustique et durabilité des composites,
458 ISTE Editions, 2018, ISBN : 978-1-78405-434-2
- 459 [5] K. Otsuka, H. Date, Fracture process zone in concrete tension specimen, *Eng. Fract.*
460 *Mech.* 65 (2000)111-131. [https://doi.org/10.1016/S0013-7944\(99\)00111-3](https://doi.org/10.1016/S0013-7944(99)00111-3)
- 461 [6] V. Kostopoulos, T. Loutas, K. Dassios, Fracture behavior and damage mechanisms
462 identification of SiC/glass ceramic composites using AE monitoring, *Compos. Sci. Technol.*
463 67(7–8) (2007) 1740–1746. <https://doi.org/10.1016/j.compscitech.2005.02.002>
- 464 [7] J. Saliba, A. Loukili, F. Grondin, J.P. Regoin, Experimental study of creep-damage in
465 concrete by acoustic emission technique, *Mater Struct.* 45(9) (2012) 1389-1401.
466 <https://doi.org/10.1617/s11527-012-9840-3>
- 467 [8] V. Munoz, B. Valès, M. Perrin, M.L. Pastor, H. Weleman, A. Cantarel, M. Karama,
468 Damage detection in CFRP by coupling acoustic emission and infrared thermography,
469 *Composites Part B* 85 (2016) 68-75. <https://doi.org/10.1016/j.compositesb.2015.09.011>
- 470 [9] M.P. Ansell, Acoustic emission from softwoods in tension, *Wood. Sci. Technol.* 16(1)
471 (1982) 35–57. <https://doi.org/10.1007/BF00351373>

- 472 [10] A. Vautrin, B. Harris, Acoustic emission characterization of flexural loading damage in
473 wood, *J. Mat. Sc.* 22(10) (1987) 3707–3716. <https://doi.org/10.1007/BF01161482>
- 474 [11] A. Reiterer, S.E. Stanzl-Tschegg, E.K. Tschegg, Mode I fracture and acoustic emission
475 of softwood and hardwood, *Wood. Sci. Technol.* 34(5) (2000) 417-430.
476 <https://doi.org/10.1007/s002260000056>
- 477 [12] Z. Chen, B. Gabbitas, D. Hunt, Monitoring the fracture of wood in torsion using acoustic
478 emission, *J. Mater. Sci.* 41(12) (2006) 3645–3655. <https://doi.org/10.1007/s10853-006-6292-6>
- 479 [13] F. Baensch, M. Zauner, S.J. Sanabria, M.G.R. Sause, B.R. Pinzer, A.J. Brunner, M.
480 Stampanoni, P. Niemz, Damage evolution in wood: synchrotron radiation micro-computed
481 tomography (SR μ CT) as complementary tool for interpreting acoustic emission (AE)
482 behavior, *Holzforschung* 69(8) (2015) 1015-1025. <https://doi.org/10.1515/hf-2014-0152>
- 483 [14] F. Lamy, M. Takarli, N. Angellier, F. Dubois, O. Pop, Acoustic emission technique for
484 fracture analysis in wood materials, *Int. J. Fract.* 192(1) (2015) 57-70.
485 <https://doi.org/10.1007/s10704-014-9985-x>
- 486 [15] M. Diakhate, E. Bastidas-Arteaga, R. Moutou-Pitti, F. Schoefs, Probabilistic
487 improvement of crack propagation monitoring by using acoustic emission, *Fracture, Fatigue,*
488 *Failure and Damage Evolution* 8 (2017)111-118. [https://doi.org/10.1007/978-3-319-42195-](https://doi.org/10.1007/978-3-319-42195-7_16)
489 [7_16](https://doi.org/10.1007/978-3-319-42195-7_16)
- 490 [16] J. Venet, R. Keller, *Identification et classement des bois français*, Second ed., ENGREF,
491 Nancy, France 1987, ISBN 978-2-857-10020-1.
- 492 [17] R.J. Ross, *Wood handbook : wood as an engineering material*, USDA Forest Service,
493 Forest Products Laboratory, General Technical Report FPL- GTR-190, (2010) 509,
494 <https://doi.org/10.2737/FPL-GTR-190>
- 495 [18] F.P. Kolmann, W.A. Côté, *Principles of Wood Sciences and Technology, Part I: solid*
496 *wood*, Springer Science&Business Media, 2012, ISBN 978-3-642-87928-9
- 497 [19] NF B51-008, *Solid wood – Static bending – Determination of ultimate strength in static*
498 *bending using small clear specimens*, AFNOR editions, 2017
- 499 [20] NF B51-002, *Standard test method for physical and mechanical characteristics of wood*,
500 AFNOR editions, 1942
- 501 [21] D. Varner, M. Cerny, M. Varner, M. Fajman, Possible sources of acoustic emission
502 during static bending test of wood specimen, *Acta Universitatis Agriculturae Mendelianae*
503 *Brunensis* 60(3) (2012) 199–206. <https://doi.org/10.11118/actaun201260030199>
- 504 [22] Y. Wu, Z.P. Shao, F. Wang, G.L. Tian, Acoustic emission characteristics and felicity
505 effect of wood fracture perpendicular to the grain, *J. Trop. For. Sci.* 26 (4) (2014) 522-531.
506 <https://www.jstor.org/stable/43150938>
- 507 [23] F. Ritschel, A.J. Brunner, P. Niemz, Nondestructive evolution of damage accumulation
508 in tensile test specimens made from solid wood and layered wood materials, *Compo. Struct.*
509 95 (2013) 44-52. <https://doi.org/10.1016/j.compstruct.2012.06.020>
- 510 [24] V. Bucur, *Acoustics of wood*, Springer Series in Wood Science, Germany, 2006, ISBN
511 978-3-540-30594-1
- 512 [25] E.N. Landis, *Acoustic Emission in Woods*, in C. Grosse, M. Ohtsu (Eds), *Acoustic*
513 *Emission Testing*, Springer-Verlag, 2008, pp. 311-322, ISBN 978-3-540-69895-1,
514 <https://doi.org/10.1007/978-3-540-69972-9>
- 515 [26] I. Yahyaoui, M. Perrin, X.J. Gong, *Damage evolution in wood under tensile loading*

516 monitored by acoustic emission, TAMAP Journals of Engineering, 2017, article ID-15,
517 http://www.tamap.org/Content/AID_15-25102017161531-.pdf

518 [27] N. Hsu, F. Breckenridge, Characterization and calibration of acoustic emission sensors,
519 *Materials Evaluation* 39 (1) (1981) 60-68

520 [28] S. Huguet, Application de classificateurs aux données d'émission acoustique :
521 identification de la signature acoustique des mécanismes d'endommagement dans les
522 composites à matrice polymère, Doctoral dissertation, INSA de Lyon, Lyon, France 2002

523 [29] A. Foulon, Détermination de la signature acoustique de la corrosion des composites SVR
524 (stratifiés verre résine), Doctoral dissertation, Technology University of Compiègne,
525 Compiègne, France, 2015

526 [30] JT. Tou, Dynoc – A dynamic optimal cluster-seeking technique, *International Journal of*
527 *Parallel Programming* 8 (6) (1979) 541-547

528 [31] J. Bodig, B. Jayne, *Mechanics of wood and wood composites*, Krieger Publishing
529 Company, 1993, ISBN 978-0-894-64777-2

530 [32] G. Pluinage, *La rupture du bois et de ses composites*, Cépaduès-Éditions, 2005, ISBN
531 978-2-85428-292-4

532 [33] S. Aicher, L. Höfflin, G. Dill-Langer, Damage evolution and acoustic emission of wood
533 at tension perpendicular to fiber, *Holz Roh und Werks.* 59(1-2) (2001) 104–116.
534 <https://doi.org/10.1007/s001070050482>

535 [34] M. Shigeishi, S. Colombo, K.J. Broughton, H. Rutledge, A.J. Batchelor, M.C. Forde,
536 *Acoustic emission to assess and monitor the integrity of bridges*, *Construction and building*
537 *materials* 15(1) (2001) 35-49